




Paper Type: Original Article



Investigation of charge carrier transport and recombination in organic semiconductors with Charge Extraction by Linearly Increasing Voltage (CELIV) technique

Ali Mahmoudloo^{1,*} ¹ Department of Basic Science, Farhangian University, Tehran, Iran, a.mahmoodlou@cfu.ac.ir;

Citation:



Mahmoudloo, A. (2022).

Investigation of charge carrier transport and recombination in organic semiconductors with Charge Extraction by Linearly Increasing Voltage (CELIV) technique. *Journal of applied research on industrial engineering*, Volume (Issue), PP.

Received: 17/01/2022

Reviewed: 20/02/2021

Revised:

Accept:

Abstract

In this article the charge extraction by linearly increasing voltage (CELIV) technique is used to calculate the drift velocity and mobility of holes in organic semiconducting polymers. The essence of this technique to measure the charge carrier mobility is very simple. The charge carrier mobility is defined as carrier drift velocity v in a given electric field E . It is a complimentary technique in the sense that it allows us to study materials when other techniques such as Time-of-Flight are inapplicable. Typically, Photo-CELIV is used to measure the charge carrier mobility in organic semiconductors since they have large bandgap (2 eV) and not many thermally generated carriers are present for extraction in the dark. The effect of recombination mechanism on the carrier mobility in the organic layer is investigated. The calculation results show that saturation of extracted charge is linearly proportional to carrier concentration at low concentrations, whereas at high density is saturated due to bimolecular carrier recombination. When Langevin recombination mechanisms are presented, the saturation of extracted charge will saturate to the capacitive displacement current step j_0 . Therefore, $\Delta j/j_0=1$ at high light intensities and the saturation of extracted charge will start to decrease from its maximum value only when t_{del} is increased to be similar to t_{max} , because in Langevin recombination the bimolecular carrier lifetime is much faster than transit time at high carrier concentrations giving the saturation of extracted charge.

Keywords: CELIV technique, organic semiconducting, charge carrier transport, time of flight




Licensee Journal of Applied Research on Industrial Engineering.

This article is an open access article distributed under the terms and conditions of the Creative Commons Attribution (CC BY) license (<http://creativecommons.org/licenses/by/4.0>).

1 | Introduction

Organic semiconductors share common features. All crystals have van-der-Waals bonded, whereas the intermolecular interactions are much weaker than the intramolecular bonds. With van-der-Waals distances of the order of 3.8 to 4Å, individual molecules are well separated. Due to the weak bonding, these materials' structural and mechanical behaviors are remarkably different from inorganic materials. For instance, hardness is usually lower than in inorganic materials, and the thermal expansion coefficients tend to be larger [1].

 Corresponding Author: a.mahmoodlou@cfu.ac.ir

 <https://doi.org/10.22105/jarie.2022.344217.1474>

Organic semiconductors mainly come in two varieties: Small molecules and polymers. Small molecules, as the name suggests, are relatively small molecular weight molecules with conjugated carbon atoms. These substances can be prepared as single molecular crystals. Due to the close coupling of the π -systems of the molecules in these crystals, they show in a purified remarkable form transport properties with mobilities of $1-10 \frac{cm^2}{VS}$. Most

molecules can be easily evaporated to form polycrystalline layers. Organic semiconducting polymers are long chains of conjugated carbon atoms that composed of smaller repeating units called monomers. The advantage of polymers is that, when modified with suitable side chains, they can be self-organize when deposited from solution at room temperature yielding a fairly high mobility layer, therefore, they can be used to print circuits at a low manufacturing cost [2],[3].

It is important to measure the fundamental limits of the charge carrier mobilities in organic semiconductors in order to develop organic electronics. Although devices such as OFETs¹, OTFTs² and OLEDs³ are already used in commercial applications. There is still no complete understanding of the final limitations of performance and stability in these devices at this time. It is necessary to determine the electronic properties in organic semiconductors for growing ultra-pure, fully ordered molecular crystals for measurements of intrinsic charge transport. The organic crystals show mobilities as high as amorphous silicon. Dislocations and grain boundaries, which may limit charge transfer, are important in these crystals [4]. Thermal expansion must be considered when devising crystal growth procedures, since the (often anisotropic) expansion tensor produces large stress/strain fields in the presence of temperature gradients. Charge carrier transport in organic semiconductors have been investigated over three decades. The most important features of the charge transport directly follow from the basic structural features of organic glasses. These glasses are molecular materials with rather weak interactions between molecules and, at the same time, they have significant disorder in position and orientations of molecules. This means that all relevant states are localized and charge carrier transport occurs by the hopping mechanism. The hopping transport is important method for disordered materials[5].

The recent success of organic light emitting diodes (OLEDs) in display technology further increases the demand for “all-organic” electronics. Indeed, it would be highly beneficial for the manufacturing process if the corresponding electronic circuitry driving the organic displays could also be made of organic material. The past decade has seen substantial progress in this field; organic molecules with extended π -conjugation have been successfully used as active semiconductors in devices like organic field effect transistors (OFETs).

It is disturbing, however, that a satisfying understanding of the physical principles governing charge transport in organic materials is still missing. Whereas in disordered polymeric organic materials a hopping-transport of, both, electrons and holes prevails, the classical experiments carried out by Karl and coworkers demonstrated the presence of a “band-like” transport mechanism for both types of charge carriers in highly ordered, ultra-pure organic single crystals of mm-sized dimensions.⁴ It is obvious, however, that the concept of band-transport successfully used to describe charge transport in conventional inorganic semiconductors like Si and GaAs is inappropriate for organic semiconductor (OSC) materials. Previous theoretical work has demonstrated that the electronic bands in OSCs are essentially flat. For such a situation the conventional description predicts very low charge carrier mobility – the figure of merit of semiconductor materials. In accord with this striking failure, recent progress in the theoretical description of charge transport in organic materials has indicated that a completely different physical picture is needed to describe charge transport in organic materials. Most importantly, lattice vibrations have to be taken into account explicitly. For ordered crystalline systems model Hamiltonians have been established, where the interaction between molecules as well as the

² organic field effect transistors

³ organic thin film transistors

⁴ organic light emitting diodes

lattice dynamic are parametrized. As systems become more disordered however, the parametrization is no longer straight forward and these methods lose their predictive power. Clearly, a precise description of charge transport phenomena requires an atomistic simulation for the true (*i.e.* including thermally vibrations) structure. There are two main approaches to this problem. One is a molecular dynamic simulation of the morphology, wherefrom charge transfer parameters can be extracted. These are then further used in hopping models to describe the movement of the localized charge from one molecule to the other. The second path is the propagation of the electronic degrees of freedom using the time dependent Schrödinger equation, whereas the cores are propagated classically with non-adiabatic simulation schemes [6].

Since charge transport in organic materials is also important to obtain a deeper understanding of organic light emitting diodes (OLED), organic solar cells and nanoscale molecular electronics, information on mobilities in organic materials as well as guiding principles to construct organic molecules with high mobilities are urgently required. Even more pressing is the need for rules with predictive power allowing for a rational design and synthesis of molecules with high charge carrier mobilities. Simplistic guiding principles like “best mobility values are obtained for planar molecules where π - π -interactions allow an optimal stacking” are valuable but are sometimes difficult to apply, *e.g.* when explaining the fact that some of the molecules showing the highest mobilities deviate substantially from planar geometries (*e.g.* rubrene). Therefore, the search for organic molecules with high charge carrier mobilities has largely remained a trial-and-error effort [7].

This paper gives a simple overview of the workings of organic photovoltaic devices, the way in which charge transfer occurs through the active layers, and then introduces how photo-induced charge carrier extraction by linearly increasing voltage (photo-CELIV) technique can be employed to give comprehensive indications of charge carrier mobility, density and recombination in organic photovoltaics. It is shown how photo-CELIV characterization, using extraction current transients, can give an understanding of degradation mechanisms through observation of the trapping of charge carriers and bimolecular recombination. Examples of deployment and the interpretation of the results are given. It is hoped that this brief introduction will serve as a stepping stone into more in-depth papers and books and encourage wider use of photo-CELIV technology which can be employed with whole devices.

2 | Calculation and Model

CELIV is powerful method allowing the charge transport and recombination to be studied in various semiconductors. It is a complimentary technique in the sense that it allows to study materials when other techniques such as Time-of-Flight are inapplicable [8].

The advantages are: 1- Strongly dispersive transport in disordered semiconductors can be probed, where in TOF¹ featureless exponential decay is seen. 2- Extraction time t_{\max} is still visible in strongly dispersive transport (in TOF the position of the kink is not so obvious even in log-log scale). 3- Films with high intrinsic conductivity can be studied, whereas in TOF only films with low conductivity can be measured. 4- Recombination processes can be studied [9], [10].

The equation to calculate charge carrier mobility in case of surface photogenerated small charge was derived:

$$t_{tr} = d\sqrt{2/\mu A}$$

(1)

Organic electronic devices, such as solar cells and light emitting diodes are typically very thin, on the order of hundreds of nanometers, therefore, charge carrier are photogenerated in the volume of the films, according to

¹ Time of flight

Beer-Lambert law. Also, charge carrier distribution due to doping is typically homogeneous throughout the film [11].

$$t_{\max} = \frac{t_{tr}}{\sqrt{3}} = d\sqrt{2/3\mu A} \quad (2)$$

The case of high conductivity, carrier extraction:

$$t_{\max} = \sqrt[3]{t_{tr}^2 \tau_{\sigma} / 2} = \sqrt[3]{\tau_{\sigma} d^2 / \mu A} \quad (3)$$

A correction factor to estimate the carrier mobility for intermediate film conductivities again in case of carrier extraction from the film was published later as determined from numerical calculations [12].

$$t_{\max} = d \sqrt{\frac{2}{3\mu A (1 + 0.36 \frac{\Delta j}{j_0})}} \quad (4)$$

Where μ is mobility of organic semiconductor, d is layer thickness, A is layer area, t_{tr} is transit time and σ is conductivity.

Further works by other groups, namely Deibel and Bange showed that the correction factor shall be slightly different, which would only change the results much less than the experimental error itself. They also demonstrated, that CELIV transients and the extraction time itself are dependent carrier bimolecular recombination and carrier concentration, which must be considered and accounted for in mobility calculations [13], [14]. We have extended this work further to account for all possible experimental parameters, namely light absorption profile, charge carrier concentration, and bimolecular recombination all together. How to calculate the charge carrier mobility in CELIV experiment correctly accounting for all these experimental conditions is discussed below.

Typical CELIV setup is not different than TOF, except that when TOF can be (though usually is not) measured with large load resistances (integral mode TOF), CELIV can only be done in differential mode when the load resistance is low ($RC < t_{tr}$) [15].

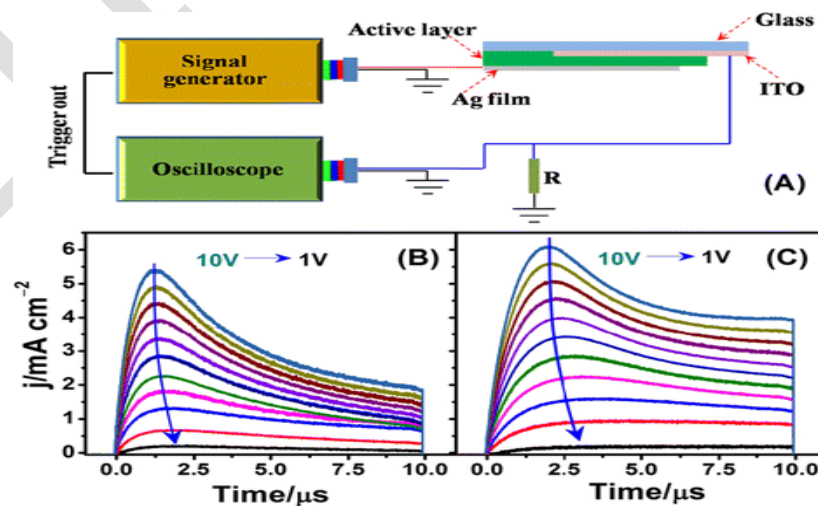


Fig.1. Schematic Experimental setup and typical CELIV transients

Triangle-shaped increasing voltage pulse is applied and the current response is measured as change in voltage on the load resistance of the oscilloscope.

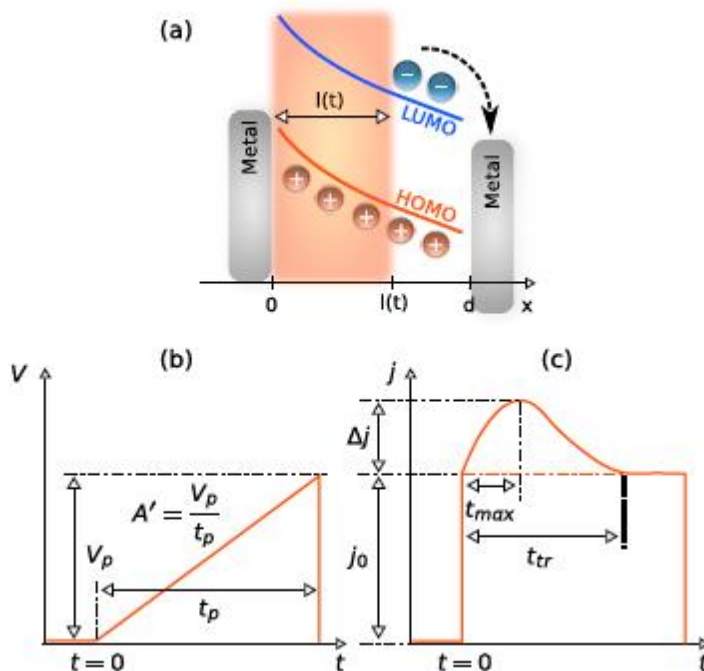


Fig. 2. Schematic illustration of the CELIV method. (a) Process of the charge extraction. (b) Scheme of the voltage input. (c) The current output.

Two types CELIV experiments can be done: [16].

1. Extraction of equilibrium generated (due to doping) carriers.
2. Extraction of photogenerated carriers, photo-CELIV. This mode is used for undoped films, when no thermally generated (equilibrium) carriers exist.

Typically, Photo-CELIV is used to measure the charge carrier mobility in organic semiconductors since they are large bandgap (2 eV or so) and not much thermally generated carriers are present for extraction in the dark [17],[18].

The essence of this technique to measure the charge carrier mobility is very simple. The charge carrier mobility is defined as carrier drift velocity v in a given electric field E :

$$v = \mu \cdot E$$

(5)

From classical mechanics, the constant speed of moving object is defined as the time required to travel the given distance d :

$$v = d / t$$

(6)

In our case, the given distance is the film thickness and time is the transit time:

$$\mu = \frac{v}{t_{tr} \cdot E} = \frac{d^2}{t_{tr} \cdot U}$$

(7)

The transit time is the time required to extract the small amount of charge carriers (less than CU) from the surface through the film. While carriers are being extracted by applied electric field, the current is observed in the external circuit and recorded in the oscilloscope. When all carriers reach the opposite electrode, extraction current drops to zero and the extraction time is recorded from which carrier mobility is calculated. However, in CELIV, the electric field is non-constant, carrier generation might be not at the surface and the time at the extraction maximum current is taken for mobility calculations, which require complex analysis. Similarly as in TOF, the mobility of both electrons and holes can be measured from CELIV. An important requirement is to

fulfill the surface carrier generation which can be done by making film thickness much larger than the photogeneration profile due to Beer-Lambert law ($d \gg ad$). As can be seen from the **Figure 3**, the extraction of either electrons or holes through the film can be chosen by applying forward or reverse bias, or, if forward bias injects shows too heavy injection, the illumination from different electrodes can be done keeping the same applied bias [19]-[21].

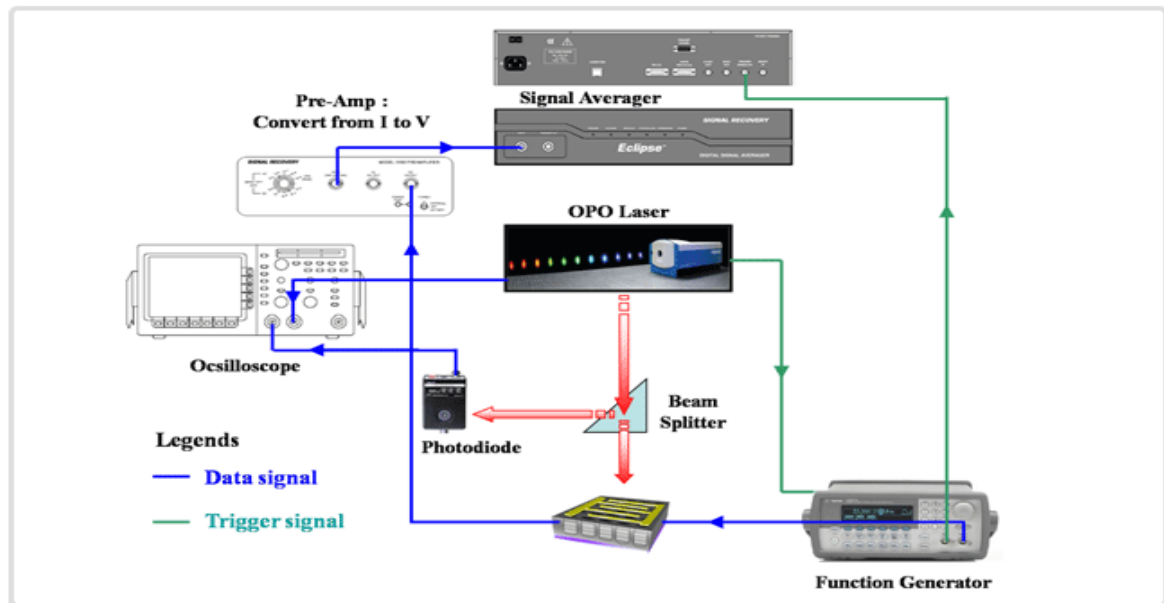


Fig. 3. Schematic measuring the mobility of electrons and holes

3 | Results and Discussion

The disadvantage of this type of experiment is that typically thick films, on the order of micrometers or more, are required. Typical thickness of organic electronic devices is much less, meaning that typically the faster carrier mobility can only be measured from CELIV in operational devices [22], [23].

Striving for universal equation to calculate the mobility of photogenerated charge carriers in all possible experimental cases, the numerical calculations were used to simulate the experimental conditions and derive the correction factor to account for:

- Light absorption profile.
- Carrier concentration.
- Langevin-type bimolecular recombination.

While no analytical solution for correction factor presently exists, the following graph can be conveniently used to correctly calculate the charge carrier mobility in systems with Langevin bimolecular charge carrier recombination (typically most materials with carrier mobility $< 1 \text{ cm}^2/\text{V}\cdot\text{s}$).

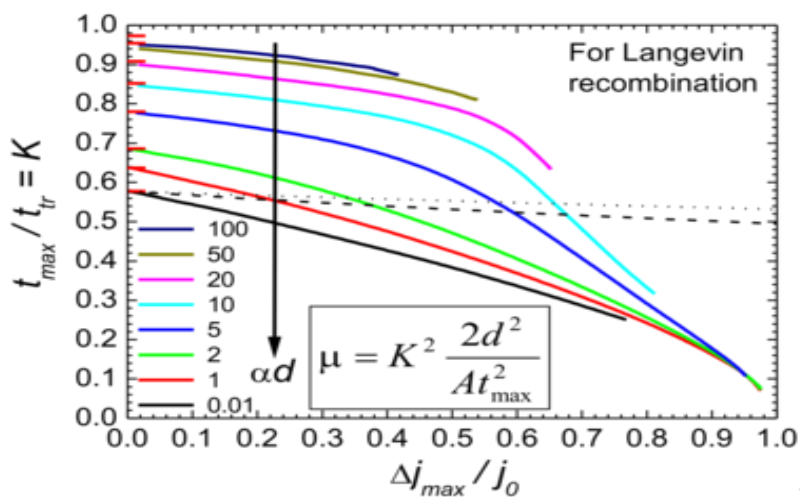


Fig. 4. Calculate charge carrier mobility with Langevin bimolecular charge carrier recombination, the Δj will saturate to the capacitive displacement current step j_0 , therefore $\Delta j/j_0=1$ at high light intensities.

The easiest way to calculate the charge carrier mobility is in boundary cases: either in very thin or thick films at low carrier concentration (small charge mode). **Figure 4** shown in this case the correction factor becomes either $K=2$ for surface photogeneration and $2/3$ for volume generation, exactly as it was shown and derived in the past.

By inserting the field dependence of mobility, we get the field dependent transport equation: [24], [25].

$$\frac{\partial}{\partial x} \left(\mu_0 \left(\frac{\beta \left(\frac{\partial V}{\partial x} \right)^2}{KT} \right) V \frac{\partial V}{\partial x} \right) = \frac{\partial V}{\partial t} \quad (8)$$

In this formulation the room temperature transient time is considered, the result of which is shown in **figure5**.

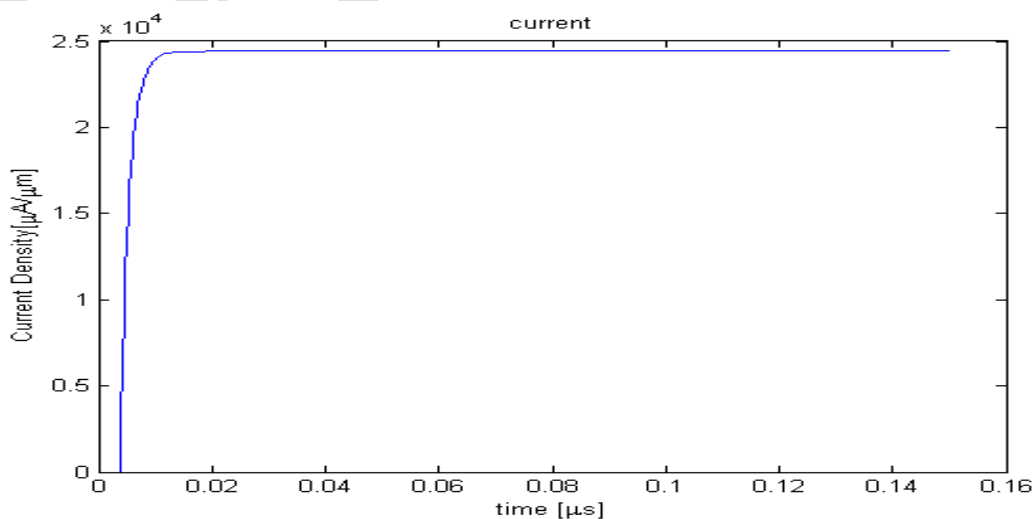


Fig. 5. Current density in simulation of transport of carriers along the organic layer

We have used a simple model consisting in a single trap level characterized by a carrier lifetime τ . The current equation is: [25], [26].

$$\frac{1}{e} \frac{\partial J_p}{\partial x} + \frac{\partial P}{\partial t} = \frac{p - p_0}{\tau} \quad (9)$$

As one of the greatest advantages of CELIV is the ability to measure the concentration of photogenerated charge carriers at various delay times or light intensities. The presence of bimolecular carrier recombination, and at what light intensity it starts to dominate, can be estimated from the **figure 6** shown below when Δj deviates from linear dependence. Unfortunately, only very rough estimate of concentration can be made.

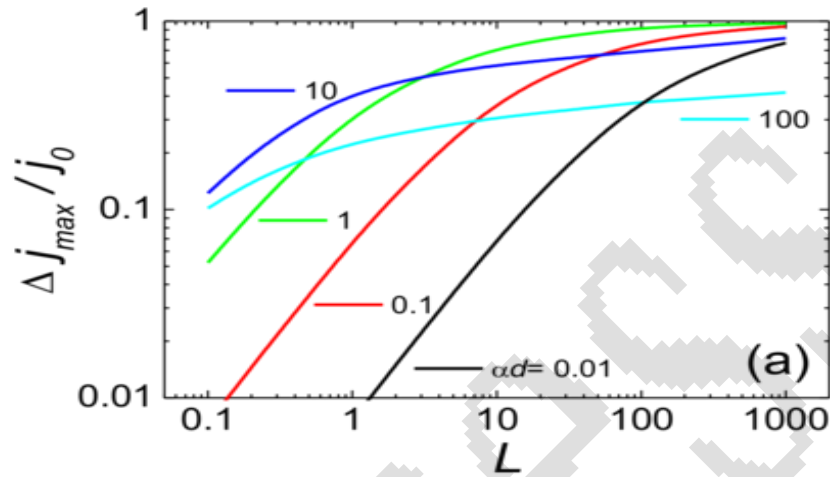


Fig. 6. Carrier lifetime and recombination measurement, the Δj will saturate to the capacitive displacement current step j_0 , therefore $\Delta j/j_0=1$ at high light intensities.

Which represents the transient response in the presence of a single trap, while the lifetime of the carriers is about 5-10 nanosecond. It can be seen that lifetimes should be larger than or equal to the delay time. This is because the holes are transported across the layer before they can get trapped. The steady state current decreases as the lifetime is reduced because of the reduction in the number of carriers that contribute to conduction by trapping.

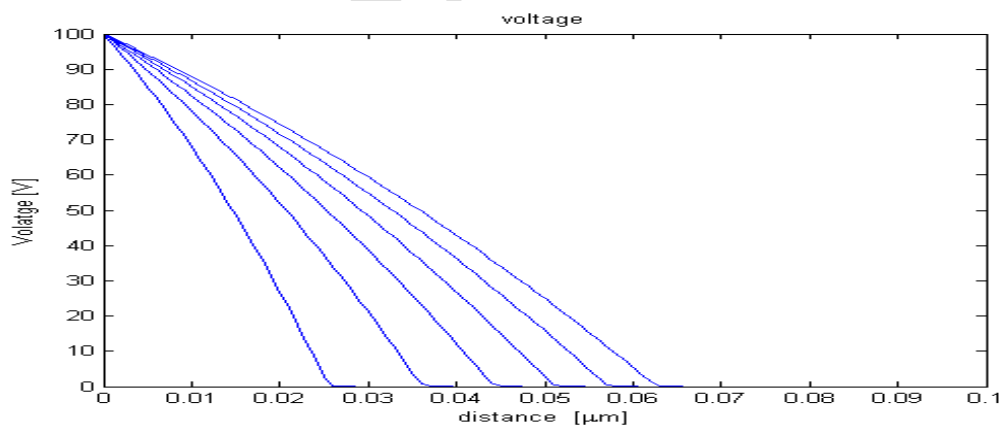


Fig. 7. Voltage behavior simulation of transport of carriers along the organic layer in intervals of 10 nanoseconds

The pulse voltage response is shown in **figure 7** along the organic layer with TOF configuration. It shows by increasing the layers thickness that the pulse voltage decays and shows a linear profile before it reaches the collector electrode.

Significant progress has been achieved in the development of novel materials and new device engineering in the last decade. In this regard, arylene diimide families have shown high promise as useful building blocks for the fabrication of next-generation electronic and optoelectronics devices, providing deeper insight into their

transistor characteristics at the molecular scale to practical applications ranging from medicine to high end security systems. These organic compounds are being developed for improved resistance to thermal and environmental stresses, which is one of the major challenges in the field. Several other classes of compounds based on fullerene (C60) and chemically modified thiophenes are also being explored and developed for use in a plethora of devices encompassing interdisciplinary research areas. These devices, owing to their low-cost, ease of synthesis and processing, are expected to pave the way for next-generation electronics with energy-efficient security systems, sensors, photonics, and spintronic memories. In this chapter we present a brief review on the different types of organic devices, their fabrication processes, and recent applications by citing examples of oligomers and polymers.

4 | Conclusions

The calculation results shows saturation of extracted charge (Δj) is linearly proportional to carrier concentration at low concentrations, whereas at high concentrations it saturates due to bimolecular carrier recombination. When Langevin recombination mechanisms is present, the Δj will saturate to the capacitive displacement current step j_0 , therefore $\Delta j/j_0=1$ at high light intensities. Experimentally this saturation can be observed by changing the delay time t_{del} or laser intensity both control the carrier concentration when the extraction pulse is applied. The saturation of extracted charge will start to decrease from its maximum value only when t_{del} is increased to be similar to t_{max} , because in Langevin recombination the bimolecular carrier lifetime is much faster than transit time at high carrier concentrations giving the saturation of extracted charge. When $t_{del} = t_{tr}$, the extracted charge will be approx= CU. This is an important observation, since it shows that only time scale $> t_{tr}$ can be probed using CELIV when measuring carrier concentration decay with time. It is not the limitation of CELIV technique, is the nature of drift governed carrier extraction from the films. Similar results would be observed in whatever electrical extraction method used (for instance using charge extraction with square-pulsed voltage).

References

- [1] Kreouzis, T., Poplavskyy, D., Tuladhar, S., Nelson J., Campbell A.J. (2016). Temperature and field dependence of hole mobility in poly(9,9-dioctylfluorene). *Phys.Rev. B.* 73(2), 801-809. <https://journals.aps.org/prb/abstract/10.1103/PhysRevB.73.020501>
- [2] Majewski, L. A., Schroeder, R., Voigt, M., Grell, M.(2014). Low voltage organic transistors on a polymer. *J. Phys. D.* 37(7), 337-347. <https://doi.org/10.1088/0022-3727/37/24/003>
- [3] Majewski, L. A., Schroeder, R., Grell, M., Turner, M. L. (2019). J. High capacitance organic field – effect transistors with modified gate insulator surface. *Appl. Phys.* 96(6), 435–447. <https://doi.org/10.1063/1.1798401>
- [4] Steudel, S., Vusser, S. D., Jonge, S. D., Janssen, D., Verlaak, S. (2015). Influence of the dielectric roughness on the performance of pentanene transistors. *Appl. Phys. Lett.* 85, 302-311. <https://doi.org/10.1063/1.1815042>
- [5] Mahmoudloo, A., Ahmadi, S. (2016). Variable range hopping transport characteristics of the charge carriers in homogenous amorphous organic semiconductors. *Optik.* 127, 505- 513. <https://www.sciencedirect.com/journal/optik/vol/127/issue/3>
- [6] Evgeny, L. Pankratov. (2022). On increasing of density of field-effect heterotransistors in the framework of a c-multiplier, *Journal of applied research on industrial engineering,* 11(2), 92-118. <http://dx.doi.org/10.22105/riej.2022.323547.1279>
- [7] Schrader, M., Körner, C., Elschner, C., Andrienko, D. (2020). Charge transport in amorphous and smectic oligothiophenes. *J. Mater. Chem.* 22, 119-124. <https://doi.org/10.1039/c2jm34837c>
- [8] Liu, C., Huang, K. (2017). A unified understanding of charge transport in organic semiconductors the importance of attenuated delocalization for the carriers. *Materials Horizons.* 4, 233-240. <https://doi.org/10.1039/c7mh00091j>
- [9] Sari, I. U., Ak, U. (2022). Machine efficiency measurement in industry 4.0 using fuzzy data envelopment analysis, *Journal of Fuzzy Extension & Applications,* 3(2), 78-89. <http://dx.doi.org/10.22105/jfea.2022.326644.1199>

- [10] Street, R., Northrup, N., Salleo, J. E. (2013). Transport in polycrystalline polymer thin – film transistors. *phy. Rev. B* , 71, 16, 337-348. <https://journals.aps.org/prb/abstract/10.1103/PhysRevB.71.165202>
- [11] Fritz S. E., Kelley T. W., Frisbie C. D.(2019). Effect of dielectric roughness on performance of pentacene TFTs with a polymeric smoothing layer. *J. Phys. Chem.B.* 109, 10574, 708-714. <https://doi.org/10.1021/jp044318f>
- [12] Shin, K., Yang, C., Yang, S. Y., Jeon, H. (2016). Effect of polymer gate dielectric roughness on pentacene field-effect transistors. *Appl. Phys. Lett.* 88, 072109, 351-362. <https://doi.org/10.1063/1.2176858>
- [13] Andrey, Y., Sosorev, M. (2020). Simple charge transport model for efficient search of high-mobility organic semiconductor crystals. *Materials & Design.* 192, 111-119. <https://www.sciencedirect.com/journal/materials-and-design/vol/192/suppl/c>
- [14] Veysel Tunc, A., De Sio, A., Riedel, D., Deschler, F., Da Como, E., Parisi, J., von Hauff, E. (2017). Molecular doping of low-bandgap-polymer: fullerene solar cells: Effects on transport and solar cells, *Org. Electron.*, 13,290- 299. <https://doi.org/10.1016/j.orgel.2011.11.014>
- [15] Panda, A., Muniz, S. M. (2022). Smart home with neural network based object detection, *Big Data and Computing Visions* , 2(1), 40 – 48. <http://dx.doi.org/10.22105/bdcv.2022.326975.1045>
- [16] Maennig, B., Pfeiffer, M., Nollau, A., Zhou, X., Leo K., Simon, P. (2018). Controlled p-type doping of polycrystalline and amorphous organic layers: Self-consistent description of conductivity and field-effect mobility by a microscopic percolation model, *Phys. Rev. B* , 64, 195-208. <https://doi.org/https://doi.org/10.1103/PhysRevB.64.195208>
- [17] Osterbacka, R., Pivrikas, A. (2017). Effect of 2-D Delocalization on Charge Transport and Recombination in Bulk-Heterojunction Solar Cells, *IEEE in Quantum Electronics*, 16, 1738-1745. <https://doi.org/10.1109/JSTQE.2010.2048746>
- [18] Gregg, B. A. (2019). Charged defects in soft semiconductors and their influence on organic photovoltaics, *Soft Matter.*, 5, 2985- 2991. <https://doi.org/https://doi.org/10.1039/B905722F>
- [19] Gregg, B.A.(2020). Transport in Charged Defect-Rich p-Conjugated Polymers, *J. Phys. Chem. C*, 113, 58-69. <https://doi.org/10.1039/d0sm01371d>
- [20] Hamidzadeh, S. M., Rezaei, M., Ranjbar-Bourani, M. (2022). A new dynamical behaviour modeling for a four-level supply chain: control and synchronization of hyperchaotic, *Journal of applied research on industrial engineering*, 9(2), 288-301. <http://dx.doi.org/10.22105/jarie.2022.314293.1400>
- [21] Stelzl, F. F., Wurfel, U., (2018). Modeling the influence of doping on the performance of bulk heterojunction organic solar cells: One-dimensional effective semiconductor versus two-dimensional donor/acceptor model, *Phys. Rev. B.*, 86, 753-761. <https://doi.org/10.1103/PhysRevB.86.075315>
- [22] Kotlarski, J. D., Koster, L. J. A., Blom, P. W. M., Lenes, M., Slooff, L. H.(2018). Combined optical and electrical modeling of polymer: fullerene bulk heterojunction solar cells, *J. Appl. Phys.* 103. 211- 220. <https://doi.org/10.1063/1.2905243>
- [23] Liang, C., Wang, Y., Li, D., Zhang, F. (2019). Modeling and simulation of bulk heterojunction polymer solar cells, *Sol. Energy Mater. Sol. Cells*, 127, 67–86. <http://dx.doi.org/10.1016/j.solmat.2014.04.009>
- [24] Rezzonico, D., Perucco, B., Knapp, E., Hausermann, R., Reinke, N. A., Muller, F., Ruhstaller, B. (2017). Numerical analysis of exciton dynamics in organic light-emitting devices and solar cells, *J. of Photonics for Energy*, 1 (2), 105- 114. <https://doi.org/10.1117/1.3528045>
- [25] Ray, B., Alam, M. A., (2019). Random vs regularized OPV: Limits of performance gain of organic bulk heterojunction solar cells by morphology engineering, *Sol. Energy Mater. Sol. Cells.* 99, 204- 213. <https://doi.org/10.1016/j.solmat.2011.11.042>